EnvIMEKO 17 - 7th IMEKO TC19 Symposium on
Environmental Instrumentation and Measurements
Aguascalientes, Mexico, August 3-4, 2017

Image Analysis Applied to a Freeze-concentration Water Purification System

José Mauricio Pardo, Ernesto Moya-Albor, Germán Ortega Ibarra and Jorge Brieva
Universidad Panamericana. Facultad de Ingeniería.
Augusto Rodin 498, México, Ciudad de México, 03920, México.
Telephone: +52 55 5482 1600 Ext. 5244
Email: {jpardo, emoya, 0163470, jbrieva}@up.edu.mx

***Abstract*— Freeze concentration is a promising water purification technology, specially due to the low levels of energy consumption when compared with other processes such as evaporation. Nevertheless, its development is still at pilot plant scale and more knowledge of the process is needed. One of the important parameters needed for design and control of the process is the growth velocity of the crystal, commonly known as the limit velocity. Above this velocity ice crystals will entrap solids and separation will not be successful. In this work, we describe a non-invasive technique to measure this limit velocity based on image analysis. Photographs were taken every 30 minutes in an experimental rig that allowed to freeze the sample unidirectionally. Back lighting was used in order to observe variations in luminosity at the samples surface. Image processing algorithms were used to segment the image, to identify the freezing front and to model its movement. Under the experimental conditions of this work, it was determined that the limiting freezing front velocity was 1.17 mm/h, which is a valuable information for the design and control of the process.**

***Index Terms*—Freeze concentration, segmentation, CIELAB color model, ice crystal identification, ice front velocity.**

I. Introduction

Freeze concentration (FC) is a separation method that is based on the solvent crystallization. The separation of solutes occur during solidification as the growing crystal expels the solids to its surroundings.

In the case of aqueous solutions, as the latent heat of water solidification is around 7 times lower than that of evaporation, FC energy consumption and environmental impact is low when compared with traditional evaporation technologies. Therefore, it is an interesting method for waste water treatment and desalination [1], [2], although its industrial implementation has not surpassed the pilot plant stage [3].

In order to obtain a successful separation, the balance between mass transfer and heat transfer must be controlled during FC; therefore the velocity of crystal growth has an upper limit [4]. Above this limit velocity impurities are entrapped because solids do not diffuse away from the crystal interface as fast as the crystal grows. Thus, this limit velocity of crystal growth is an important parameter for design and control of this separation process and needs to be quantified. A common practice is to measure freezing curves at different position of the sample in order to quantify this velocity.

Image processing is a continuous developing area related with the methods and algorithms used to process digital images through a computer. These methods can be classified in low-level, mid-level and higher-level processing. Low-level processes perform primitive operations such as noise reduction, image visual enhancement and sharpness restoration. Mid-level processing involves segmentation, characterization and classification of regions. High-level processes give meaning of the set of recognized regions (objects and background), in the previous levels, allowing a cognitive interpretation of this information by the computer [5].

For the FC method, image processing techniques can be an non-invasive alternative method to quantify the velocity of crystal growth, by extracting visual information from an image sequence that capture the growing crystal. Some steps involved in the visual information extraction include tasks such as: color and intensity analysis, segmentation of regions of interest, characterization and identification of the objects. Several works are developed for ice analysis in an image processing context at both macroscopic and microscopic levels. For SAT images applications, Beaven et al. estimate the ice sea concentration [6] and Bell et al. [7] estimate the trajectories of the ice in a geographical context. Microscopic image analysis has been used for the detection of the interface in freezing solutions and morphology of the crystal [8], [9].

This paper describes a non invasive technique that was developed in order to follow the movement of the ice front and to quantify its velocity using image analysis techniques at macroscopic level. The rest of the paper is organized as follows: Section II describes the experimental setup and the image processing methods, Section III presents the results and their analysis, finally Section IV concludes the paper and presents future work.

II. Materials and Methods

A. Experimental Setup

An acrylic crystallizer was built in order to freeze the sample uni-directionally. Figure 1 shows the configuration of the device. The heat sink was maintained at –15°C by recirculating ethylene-glycol at this temperature.

According to the Fourier law, Eq. 1, in steady state conditions, the speed of formation of ice and consequently the freezing front velocity in this device is expected to decrease as

978-92-990075-8-7

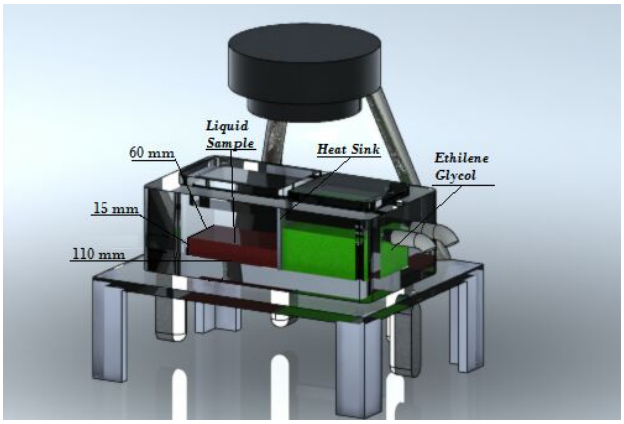

Fig. 1. Experimental rig for image acquisition.

ice front moves away from the heat sink during the experiment, therefore at some point the limit velocity is achieved.

$$q_i = -k\frac{dT}{dx} \tag{1}$$

where q_i is the heat heat flux, k is thermal conductivity of the frozen sample and dT/dx is the thermal gradient between the ice front and the heat sink.

Additionally, from the heat and mass balance q_i can be expressed as:

$$q_i = \rho_i \frac{dx}{dt} h_i \tag{2}$$

where ρ_i is density of ice, h_i is the latent heat of solidification and t is time.

The crystallizer was illuminated using back lighting and pictures of the sample where taken every 30 minutes with a digital Camera Sony DSC QX10.

B. Freezing Protocol

Ethylene glycol was circulated through the heat sink in order to cool down the crystallizer. A thin film of pure water was allowed to crystallize on the metallic surface in order to avoid undercooling of the sample. Afterwards an 80 ml sample of coffee solution with a concentration of 1 Bx was poured in the crystallizer and covered with an acrylic top. Coffee solids were used in order to increase the contrast between the pure ice and the solution. Back lighting and camera were turned on in order to follow the movement of the ice front during 12 hours.

C. Image Processing

In order to model the ice front velocity behaviour from the RGB images we performed an analysis of these in the CIE $L*a*b*$ (CIELAB) color space.

CIELAB is a system devised by the International Commission on Illumination (CIE) in 1976 [10]. The three components of this model, indicate lightness $L*$ (from 0 to 100, black and white respectively), $a*$ (from red to green) and $b*$ (from yellow to blue). The coordinate $(0, 0, 0)$ represent an achromatic center, outside of the center color saturation increases.

An approach to detect the ice front is by using the $L*$ component, therefore, we took eight sample images in a neighborhood corresponding to the region of the pure crystal. Later, we calculated the normalized histogram to find the suitable threshold of the $L*$ component in all images to isolate the region of the pure ice from the rest of the image.

A row scanning strategy was used to extract the edge corresponding to ice front position. Once the pure crystal was identified and the position of the ice front quantified in each image, a quadratic equation was adjusted to describe the position of the freezing front in each row (R) of the image as follows:

$$x_i = aR^2 + bR + c \tag{3}$$

where x_i is the position of the freezing front calculated from the heat sink the image, a,b and c are constant empirical values.

Finally, the movement of the freezing front was adjusted to the equation of the form $x_i(t) = d\sqrt{t} + \epsilon$, which is the typical form of the freezing front displacement with a constant heat sink temperature [11]. Therefore the following empirical equation was used to describe the changing position of each pixel of the ice front.

$$x_i(R,t) = \left(a_1R^2 + b_1R + c_1\right)\sqrt{t} + \left(a_2R^2 + b_2R + c_2\right) \tag{4}$$

And its velocity calculated from the following:

$$\frac{dx_i}{dt} = \frac{a_1R^2 + b_1R + c_1}{2\sqrt{t}} \tag{5}$$

III. Results and Discussion

In total 72 RGB images were obtained from three experiments to model the growth of the ice front. In Fig. 2 we show eight images obtained each 30 minutes, here we can see the displacement of the ice front and the formation of pure crystal.

Figure 3 shows the $L*a*b*$ components and their normalized histograms of the image in the time t_3 of the Fig. 2. In these kind of experiments, with backlighting, optical property of translucency is very important because the light source affects directly over the solution regions and the pure ice. In the pure ice region the light passes more easily than in regions that contains solids. Thus, the $L*$ component that represents the luminance or lightness in the scene is more relevant than components $a*$ and $b*$ in order to define the pure ice region.

Figure 4a shows the normalized histogram of the $L*$ component obtained from all sample images. This component was used to define the threshold whose value was 60. It was chosen in such a way that 97% of the pixels represent pure crystal region. Using the obtained threshold, we segmented the $L*$ component image in two regions (white correspond to ice region) as can be seen in Fig. 4b. When the threshold was applied to all the images, it was evident that ice crystal started to appear at 3.5 hours after initiating the experiment. Thus, the equation fitting was done with 8 samples obtained between 3.5 and 7.5 hours.

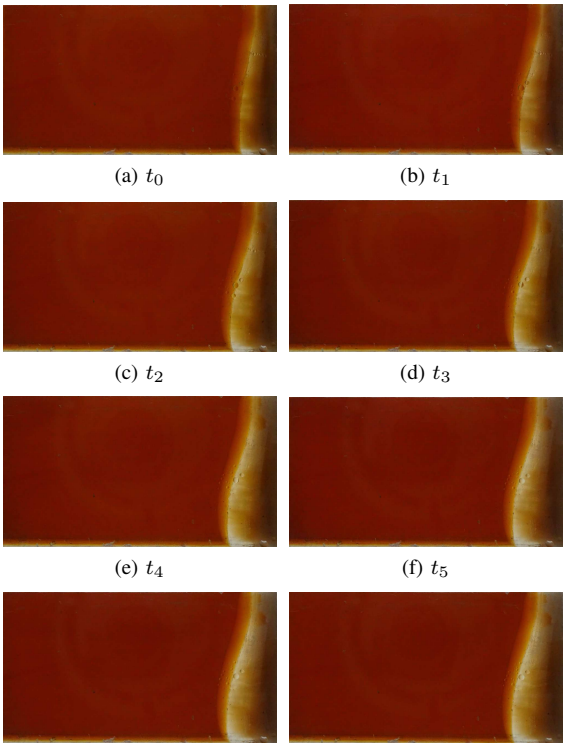

(a) t_0 (b) t_1 (c) t_2 (d) t_3 (e) t_4 (f) t_5 (g) t_6 (h) t_7

Fig. 2. RGB images obtained with a sampling period of 30 minutes.

In general terms the proposed segmentation procedure and the empirical Eq. 3 described closely the position of the ice front in a single photograph (Fig. 5a,b); in all cases

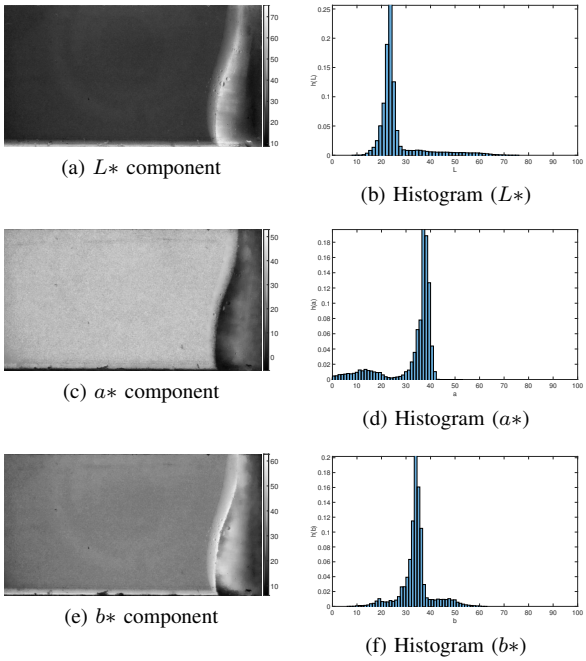

(a) $L*$ component (b) Histogram ($L*$) (c) $a*$ component (d) Histogram ($a*$) (e) $b*$ component (f) Histogram ($b*$)

Fig. 3. Example of CIELAB components of an acquired image.

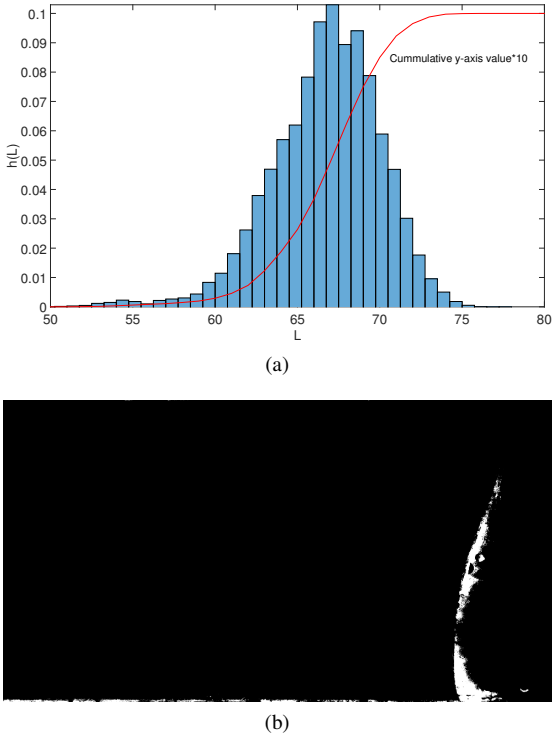

(a)

(b)

Fig. 4. Normalized histogram (and cumulative histogram in red) of the $L*$ component from ice region in all image samples (a). Segmented image using the threshold $L* = 60$.

TABLE I
EMPIRICAL PARAMETERS OF EQ. 4

	a_1	b_1	c_1
Trial 1	1.32×10^{-6}	-6.42×10^{-3}	$1.28\times10^{+1}$
Trial 2	4.80×10^{-6}	-2.26×10^{-2}	$3.10\times10^{+1}$
Trial 3	2.24×10^{-6}	-6.52×10^{-3}	$9.17\times10^{+0}$
	a_2	b_2	c_2
Trial 1	-7.61×10^{-6}	3.93×10^{-2}	$-4.18\times10^{+1}$
Trial 2	-1.45×10^{-5}	7.59×10^{-2}	$-9.35\times10^{+1}$
Trial 3	-6.81×10^{-6}	2.24×10^{-2}	$-1.15\times10^{+1}$

the correlation coefficients where above 0.98 showing the goodness of this equation to describe even the border effects.

On the other hand, Table I resumes the parameters of the empirical Eq. 4 found to describe the movement of ice front for each experiment.

As it has been mentioned before, these equations include the parameter R in millimetres and parameter t that is time in hours. In order to obtain an average velocity, the equation was evaluated in the 1000 pixels positioned around the center of each image.

Table II, shows the estimated ice front velocities of the 1000 pixels around the central rows of each trial. These velocities were estimated at 3.5 hours, which is the time where the formation of a pure crystal was identified. The average values between samples are close as expected, however the velocities range in all experiments was between 1.17 and 2.09, thus the

TABLE II
FREEZING FRONT LIMIT VELOCITIES IN MM/H.

	Average (Std. dev.)	Min	Max
Trial 1	1.39 (0.06)	1.34	1.54
Trial 2	1.32 (0.16)	1.17	1.76
Trial 3	1.55 (0.26)	1.21	2.09

higher velocity is almost twice the lower. Nevertheless, under this conditions in order to achieve the formation of a pure crystal, the velocity 1.17 mm/h is to be picked as the limit velocity.

Once the limit velocity is quantified, a heat sink temperature profile can be obtained including it as constant velocity in the heat and mass balance Eq. 1 and Eq. 2 under steady state behaviour as follows in Eq. 6:

$$T_s = T_i - \frac{\rho_i h_i}{k} V_l x_i \tag{6}$$

where, T_s and T_i are the sink and ice front temperatures respectively and V_l is the limit velocity. This equation can be easily included in a control strategy of the FC process. However, we know that this is a simple model and still contain several assumptions such as constant ice front temperature, physical properties, concentration of the unfrozen solution . In a future work, the influence of this assumptions on the temperature profile will be contrasted with experimental data. However, at this point we can conclude that the computer vision procedure used to quantify the limit velocity was successful and can be easily included in a control strategy of the process.

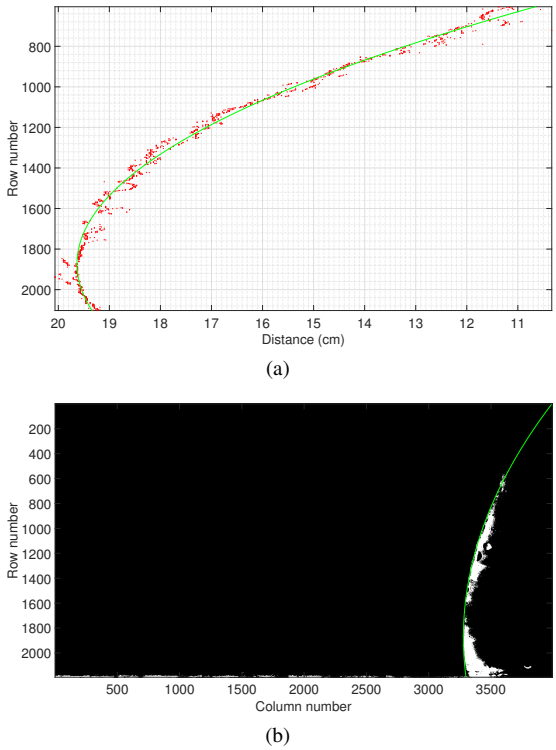

(a)

(b)

Fig. 5. Position of the ice front, red dots experimental measurements, green line fitted curve (3).

IV. CONCLUSION

A computer vision system that included image acquisition and analysis was used successfully in the measurement of the limit velocity of a freeze concentration process. The segmentation procedure using the $L*$ component from the CIEL*a*b* color space was useful to observe the formation of pure ice crystal and to quantify the position of the freezing front. Under the experimental conditions it was determined that the limiting velocity of the freezing front 1.17 mm/h which is a valuable information for the Freeze concentration process design and control.

ACKNOWLEDGMENT

Mauricio Pardo, Ernesto Moya-Albor, Germán Ortega and Jorge Brieva, would like to thank the Facultad de Ingeniería of Universidad Panamericana for all support in this work.

REFERENCES

[1] F. Belén, J. Sánchez, E. Hernández, J. Auleda, and M. Raventós, "One option for the management of wastewater from tofu production: Freeze concentration in a falling-film system," *Journal of Food Engineering*, vol. 110, no. 3, pp. 364–373, 2012.

[2] S. Badawy, "Laboratory freezing desalination of seawater," *Desalination and Water Treatment*, vol. 57, no. 24, pp. 11 040–11 047, 2016.

[3] P. M. Williams, M. Ahmad, B. S. Connolly, and D. L. Oatley-Radcliffe, "Technology for freeze concentration in the desalination industry," *Desalination*, vol. 356, pp. 314 – 327, 2015, state-of-the-Art Reviews in Desalination.

[4] X. Gu, T. Suzuki, and O. Miyawaki, "Limiting partition coefficient in progressive freeze-concentration," *Journal of Food Science*, vol. 70, no. 9, pp. E546–E551, 2005.

[5] R. C. Gonzalez and R. E. Woods, *Digital Image Processing (3rd Edition)*. Upper Saddle River, NJ, USA: Prentice-Hall, Inc., 2006.

[6] S. G. Beaven, S. Gogineni, and F. D. Carsey, "Fusion of satellite active and passive microwave data for sea ice type concentration estimates," *IEEE Transactions on Geoscience and Remote Sensing*, vol. 34, no. 5, pp. 1172–1183, Sep 1996.

[7] T. Bell, R. Briggs, R. Bachmayer, and S. Li, "Augmenting inuit knowledge for safe sea-ice travel 2014; the smartice information system," in *2014 Oceans - St. John's*, Sept 2014, pp. 1–9.

[8] B. Vemuri, K. Diller, L. Davis, and J. Aggarwal, "Image analysis of solid-liquid interface morphology in freezing solutions," *Pattern Recognition*, vol. 16, no. 1, pp. 51 – 61, 1983.

[9] C. Neils and K. Diller, "An optical-axis freezing stage for laser-scanning microscopy of broad ice-water interfaces," *Journal of Microscopy*, vol. 216, no. 3, pp. 249–262, 2004.

[10] CIE, "Cie 1976 l*a*b* color space," International Commission on Illumination, Standard, 2007.

[11] J. Pardo and K. Niranjan, *Food Processing Handbook*. Wiley-VCH Verlag GmbH & Co. KGaA, 2011, vol. 2, ch. Freezing, pp. 131–152.